Electric Power Components and Systems, 34:1163–1175, 2006

ISSN: 1532-5008 print/1532-5016 online
DOI: 10.1080/15325000600698290

Taylor & Francis
Taylor & Francis Group

Cost-Effective Control Scheme for Reduction of Torsional Torque Oscillations in Starting Large Induction Motors

NASER M. B. ABDEL-RAHIM

Electrical Engineering Department
Faculty of Engineering at Shoubra, Benha University
Cairo, Egypt

A. SHALTOUT

Electrical Power & Machines Department
Cairo University
Giza, Egypt

This article presents a cost-effective variable frequency drive for starting and operating large three-phase squirrel cage induction motors. The proposed drive employs the constant V/F control scheme, which regulates the rotor frequency such that it is always kept below a predetermined value. This has the effect of drastically reducing the motor shaft torque oscillations and significantly limiting the maximum value of the motor line current. In addition to its simplicity and hence cost-effectiveness, the proposed scheme is shown to be capable of (i) reducing the shaft torque oscillations to approximately 22% of that of the direct on-line start of the large motor, and (ii) limiting the motor line current to approximately 36% of that of the direct on-line start value.

Keywords large induction motors, motor drive, slip frequency control, constant V/F control scheme

1. Introduction

In the starting process of large induction motors (IMs) and large synchronous motors started as IMs, two problems evolve: high starting current and shaft torque oscillations. High starting current has many drawbacks, e.g., potential adverse effects, especially on weak utility networks and a drop in the motor terminal voltage, which, in turn, reduces the motor starting and accelerating torques. As for the shaft torque oscillations, they may reach hazardous levels that could lead to cyclic fatigue fracture of the shaft torque.

One of the techniques proposed to reduce the high starting current involved voltage reduction of the motor terminals [1]. This was achieved by inserting a series reactor between the motor and the utility network during the starting period. Alternatively, reduction

Manuscript received in final form on 14 March 2006.
Address correspondence to Prof. Naser Abdel-Rahim, Electrical Engineering Department, Faculty of Engineering at Shoubra, 108 Shoubra Street, Cairo, Egypt. E-mail: n_abdelrahim@yahoo.com

of the motor terminal voltage was achieved by supplying the motor through an autotransformer [1]. After the starting period was over, the series reactor, or the autotransformer, was bypassed. Although the above two techniques were successful in reducing the motor starting current, they yielded reduced starting and accelerating torques which, in turn, resulted in a prolonged starting period, which led to motor overheating.

A third technique for reducing the motor starting current was the capacitor-start method [2]. In that method, an energized capacitor was connected at the time of the motor startup period, thus providing the reactive current drawn by the motor and supporting the utility voltage. Upon reaching rated speed, the capacitor was switched off. That method, however, added to the risk of transient over-voltage and harmonic resonance.

Reduction of the shaft torque oscillations during startup with an autotransformer or star/delta switching has been achieved by the proper choice of the switching instant, as improper switching may reinitiate the shaft torque oscillations [3].

Another technique for suppressing the shaft torque oscillations was through using the slip frequency control (SFC) [4]. That control scheme employed two nested feedback loops; namely, an inner current loop and an outer speed feedback loop. Although the SFC scheme has been successful in drastically reducing the oscillations in the shaft torque and in limiting the motor starting current to a preset value, it necessitated the use of two current sensors, which resulted in higher system cost.

In the present work, it is proposed to use the constant V/F control scheme as an alternative control strategy for reduction of the oscillations in the shaft torque and for limiting the motor starting current to a maximum of 2.0 p.u. The constant V/F control scheme is advantageously cost-effective since it does not require any sensing of the line current; hence, it is simple to implement. The performance of the large three-phase IM system using constant V/F control scheme has not yet been reported in the literature.

2. Model of Large Motor System

Figure 1 shows the layout of the large motor system. It consists of a large squirrel cage induction machine driving a high inertia load through an elastic shaft. The electrical model of the motor in the stationary frame of reference is given by [5]:

$$\begin{bmatrix} \frac{x_{ss}}{\omega_o} & 0 & \frac{x_m}{\omega_o} & 0 \\ 0 & \frac{x_{ss}}{\omega_o} & 0 & \frac{x_m}{\omega_o} \\ \frac{x_m}{\omega_o} & 0 & \frac{x_{rr}}{\omega_o} & 0 \\ 0 & \frac{x_m}{\omega_o} & 0 & \frac{x_{rr}}{\omega_o} \end{bmatrix} \begin{bmatrix} \dot{i}_{qs} \\ \dot{i}_{ds} \\ \dot{i}_{qr} \\ \dot{i}_{dr} \end{bmatrix} = \begin{bmatrix} -r_s & 0 & 0 & 0 \\ 0 & -r_s & 0 & 0 \\ 0 & \frac{\omega_m}{\omega_o} x_m & -r_s & \frac{\omega_m}{\omega_o} x_{rr} \\ -\frac{\omega_m}{\omega_o} x_m & 0 & -\frac{\omega_m}{\omega_o} x_{rr} & -r_r \end{bmatrix} \begin{bmatrix} i_{qs} \\ i_{ds} \\ i_{qr} \\ i_{dr} \end{bmatrix} + \begin{bmatrix} V_{qs} \\ V_{ds} \\ 0 \\ 0 \end{bmatrix} \tag{1}$$

where

$$x_{ss} = x_s + x_m, \qquad x_{rr} = x_r + x_m, \tag{2}$$

and

i_{qs} is the quadrature component of the stator current,
i_{ds} is the direct component of the stator current,
i_{qr} is the quadrature component of the rotor current,
i_{dr} is the direct component of the rotor current,
ω_m is the motor angular speed of rotation,
ω_o is the nominal supply synchronous speed,
x_m is the motor magnetizing reactance,
x_s is the stator leakage reactance,
x_r is the rotor leakage reactance,
r_s is the stator resistance, and
r_r is the rotor resistance.

The developed electromagnetic torque, T_e, is given by

$$T_e = x_m(i_{qs}i_{dr} - i_{qr}i_{ds}) \tag{3}$$

The equation of motion of the rotating mass including the torsional dynamics of the shaft is given by [3]:

$$\begin{bmatrix} \dot{\omega}_m \\ \dot{\theta}_m \\ \dot{\omega}_l \\ \dot{\theta}_l \end{bmatrix} = \begin{bmatrix} -\dfrac{(D_m + D_{ml})}{2H_m} & -\dfrac{K_s\omega_o}{2H_m} & \dfrac{D_{ml}}{2H_m} & \dfrac{K_s\omega_o}{2H_m} \\ 1 & 0 & 0 & 0 \\ \dfrac{D_{ml}}{2H_l} & \dfrac{K_s\omega_o}{2H_l} & -\dfrac{(D_l + D_{ml})}{2H_l} & -\dfrac{K_s\omega_o}{2H_l} \\ 0 & 0 & 1 & 0 \end{bmatrix} \begin{bmatrix} \omega_m \\ \theta_m \\ \omega_l \\ \theta_l \end{bmatrix} + \begin{bmatrix} \dfrac{\omega_o}{2H_m} & 0 \\ 0 & 0 \\ 0 & -\dfrac{\omega_o}{2H_l} \\ 0 & 0 \end{bmatrix} \begin{bmatrix} T_e \\ 0 \\ T_l \\ 0 \end{bmatrix} \tag{4}$$

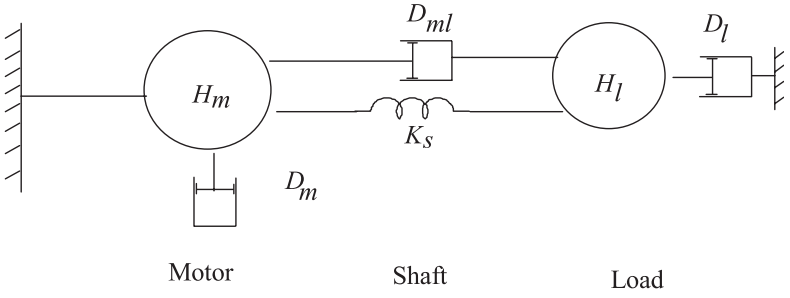

Figure 1. Layout of the large motor system.

where

θ_l is the load angular position,
θ_m is the motor angular position,
ω_l is the load angular speed of rotation,
K_s is the stiffness coefficient of the motor shaft,
H_m is the motor inertia,
D_m is the viscous friction coefficient of the motor,
D_{ml} is the mutual damping coefficient,
H_l is the load inertia,
D_l is the viscous friction coefficient of the load shaft, and
T_l is the load torque.

Equations (1) to (4) were employed to simulate the behavior of the large motor system using MATLAB/SIMULINK [6].

3. Analysis of Starting Period

This section offers a comprehensive overview of the production of various torque components of the large motor during its starting phase when fed by a sinusoidal supply and when fed by a non-sinusoidal (square wave) supply.

3.1. Sinusoidal Supply

The time response of the motor under study when the utility full voltage is applied at the motor terminals is shown in Figure 2 (the data are given in the appendix). Figure 2a shows that the developed electromagnetic torque has a decaying oscillatory component

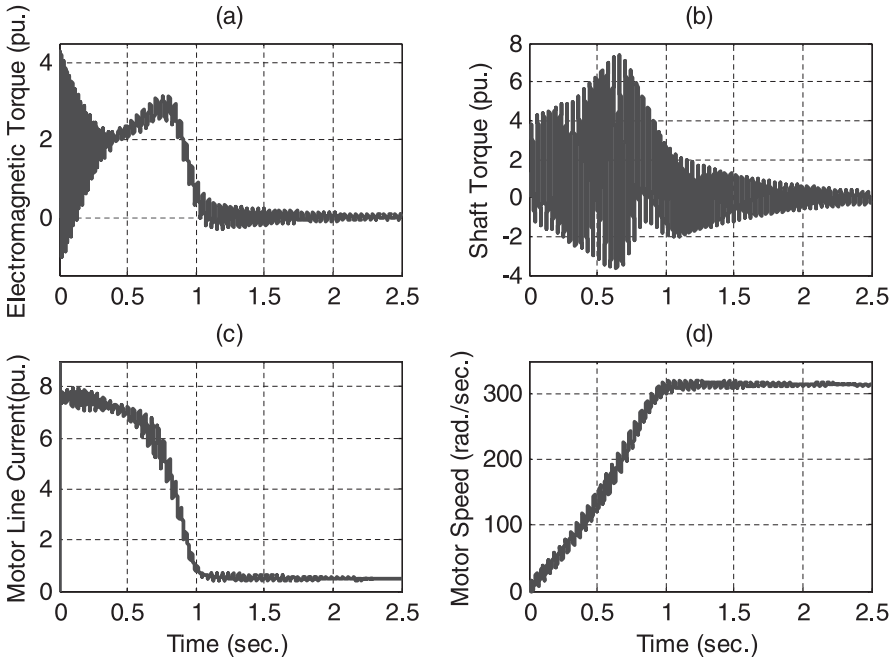

Figure 2. Motor behavior for direct on-line start.

at the supply frequency. However, as shown by Figure 2b, the shaft torque oscillates at a frequency different from that of the developed torque and such shaft torque oscillations could reach hazardous levels as high as 7.34 p.u. While the electromagnetic torque oscillations diminish, the shaft oscillations continue to build up to a certain degree.

Figure 2c shows that the motor staring current could reach as high as 7.9 p.u. The motor speed is depicted in Figure 2d, where it is shown that the motor reaches its steady-state operating speed after approximately 1 sec.

To explain the nature of the torque response, it should be noted that the sudden application of the supply produces transient currents with AC and DC components at both stator and rotor windings. As shown in Figure 3, these currents produce the following MMFs in the motor air gap [3]:

1. $\boldsymbol{M_{ss}}$, supply frequency stator MMF rotates with synchronous speed (ω_s),
2. $\boldsymbol{M_{os}}$, stationary stator MMF produced with the stator DC current, i.e. $\omega = 0$,
3. $\boldsymbol{M_{or}}$, rotor MMF produced with the DC rotor current, rotates with rotor speed (ω_m),
4. $\boldsymbol{M_{sr}}$, rotor MMF produced with the slip frequency rotor current, rotates with the synchronous speed (ω_s).

The interaction of $\boldsymbol{M_{ss}}$ and $\boldsymbol{M_{sr}}$ produces the main unidirectional component of the torque. The interaction of $\boldsymbol{M_{sr}}$ and $\boldsymbol{M_{os}}$ produces the supply frequency component of the torque. The interaction of $\boldsymbol{M_{ss}}$ and $\boldsymbol{M_{or}}$ produces a torque [slip frequency torque (SFT)] with a slip frequency of $s \times f_s$. The interaction of $\boldsymbol{M_{os}}$ and $\boldsymbol{M_{or}}$ produces a torque with a speed frequency of $(1 - s) \times f_s$.

The speed frequency component has a small magnitude and can usually be neglected [3]. Nevertheless, it is the SFT that is responsible for the high shaft torque oscillations. This component starts with the supply frequency at $s = 1$ and continues to decrease as the motor speeds up. This is demonstrated by torque building up as the slip frequency approaches the torsional frequency. A maximum value is encountered when the motor speed reaches 166 rad/sec ($s = 0.47$). This gives $s \times f_s = 23.6$ Hz, which is the same as the natural torsional frequency of the mechanical system calculated by Eq. (5) [3, 7].

$$f_t = \frac{1}{2\pi}\sqrt{\frac{K_s\omega_o}{\dfrac{2H_mH_L}{H_m + H_L}}}\ \text{Hz} \tag{5}$$

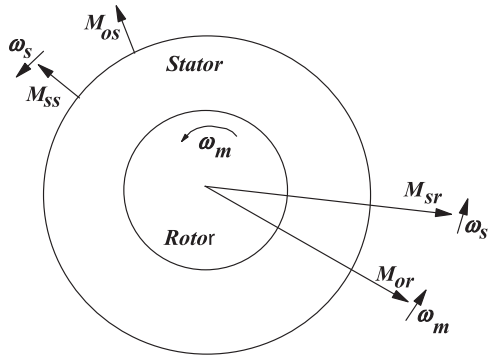

Figure 3. MMFs produced in the air gap by sinusoidal supply.

However, as the motor speed continues to grow, the slip frequency departs from the natural frequency and the shaft torque starts to decay. The aforementioned analysis has been confirmed in [4], where it was shown that the frequency spectrum of the developed torque comprises two components; namely, the unidirectional component, which produces the speed acceleration, and the SFT. The latter results in magnified shaft torque oscillations when it coincides with the natural torsional frequency.

3.2. Square Wave Supply

This subsection offers an explanation of the production of various torque components when the large motor is fed by a non-sinusoidal supply. The type of non-sinusoidal supply chosen here is the square-wave supply, which has the advantage of producing a predefined frequency spectrum at the motor terminals, allowing for straightforward explanation of the motor behavior.

For a Y-connected motor fed from a square wave voltage supply, the stator current contains the fundamental and non-triple-n odd harmonic components. The fundamental current produces torque components similar to those of the sinusoidal supply. The 5th harmonic current produces an MMF, $\boldsymbol{M_{5s}}$, which rotates with speed $5\omega_s$ in the opposite direction of the fundamental component. This component produces a current in the rotor conductors with a frequency of $(6-s)f_s$. The induced current produces an MMF, $\boldsymbol{M_{5r}}$, which rotates with speed $(6-s)\omega_s$ with respect to the rotor conductors and with speed $5\omega_s$ in space. These additional MMF components are illustrated in Figure 4. The interaction of these additional MMFs produces the following torque components:

1. $\boldsymbol{M_{5s}}$ interacts with $\boldsymbol{M_{5r}}$ to produce a unidirectional torque, which is an opposing torque.
2. $\boldsymbol{M_{5s}}$ interacts with $\boldsymbol{M_{sr}}$ to produce a torque with $6f_s$ frequency.
3. $\boldsymbol{M_{5s}}$ interacts with $\boldsymbol{M_{or}}$ to produce a torque with $(6-s)f_s$ frequency.
4. $\boldsymbol{M_{5r}}$ interacts with $\boldsymbol{M_{ss}}$ to produce a torque with $6f_s$ frequency.
5. $\boldsymbol{M_{5r}}$ interacts with $\boldsymbol{M_{os}}$ to produce a torque with $5f_s$ frequency.

The 7th harmonic current produces an MMF $\boldsymbol{M_{7s}}$ which rotates with speed $7\omega_s$ in the forward direction. This component produces a rotor current in the rotor conductor with a frequency of $(7-s)f_s$. The induced current produces an MMF $\boldsymbol{M_{7r}}$ which rotates

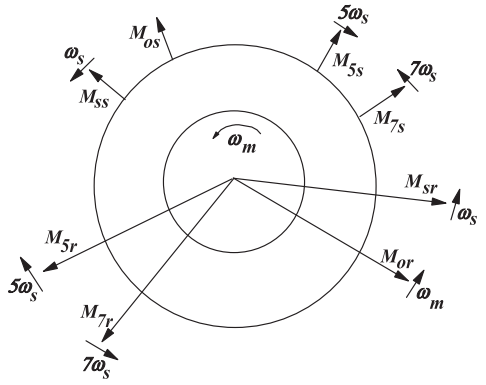

Figure 4. MMFs produced in the air gap by non-sinusoidal supply.

with speed $(7 - s)\omega_s$ with respect to the rotor conductors and with speed $7\omega_s$ in space (see Figure 4).

The 7th harmonic component produces the following torques:

1. $\boldsymbol{M_{7s}}$ interacts with $\boldsymbol{M_{7r}}$ to produce a unidirectional torque component in the forward direction (aiding torque).
2. $\boldsymbol{M_{7s}}$ interacts with $\boldsymbol{M_{sr}}$ to produce a torque with a frequency $= 6f_s$.
3. $\boldsymbol{M_{7s}}$ interacts with $\boldsymbol{M_{or}}$ to produce a torque with a frequency $= (6 + s)f_s$.
4. $\boldsymbol{M_{7s}}$ interacts with $\boldsymbol{M_{5r}}$ to produce a torque with a frequency $= 12f_s$.
5. $\boldsymbol{M_{7r}}$ interacts with $\boldsymbol{M_{ss}}$ to produce a torque with a frequency $= 6f_s$.
6. $\boldsymbol{M_{7r}}$ interacts with $\boldsymbol{M_{os}}$ to produce a torque with a frequency $= 7f_s$.
7. $\boldsymbol{M_{7r}}$ interacts with $\boldsymbol{M_{5s}}$ to produce a torque with a frequency $= 12f_s$.

It can, thus, be concluded that during the starting period, the 5th and 7th harmonic currents produce torque components with $12f_s$ as well as torque components in the frequency band $5f_s$ to $7f_s$. At the end of the starting period, the transient components $\boldsymbol{M_{os}}$ and $\boldsymbol{M_{or}}$ decay while only the $5f_s$ to $7f_s$ and $12f_s$ components remain. The $12f_s$ component has high frequency and will be ignored in this study. On the other hand, torque components in the frequency band $5f_s$ to $7f_s$ Hz, in the system under study, is far from its natural torsional frequency. Therefore, they only have minimal impact on the shaft torque. However, when the motor is started with variable frequency inverter (where the frequency is gradually increased) the $5f_s$ to $7f_s$ torque components may coincide with the natural torsional frequency at low values of f_s, and hazardous torsional torques will be encountered. Therefore, special care has to be exerted to examine the problem and alleviate its impact in inverter-fed large induction motors.

In order to control the frequency of the SFT component, a static voltage-source inverter is used to control both the motor terminal voltage and its frequency. Investigation of the motor performance using the constant V/F control scheme is presented in the next section.

4. Constant V/F Control Scheme

Figure 5 shows the constant V/F control scheme of the variable frequency drive of the large motor system. The power circuit consists of a three-phase bridge rectifier, a second

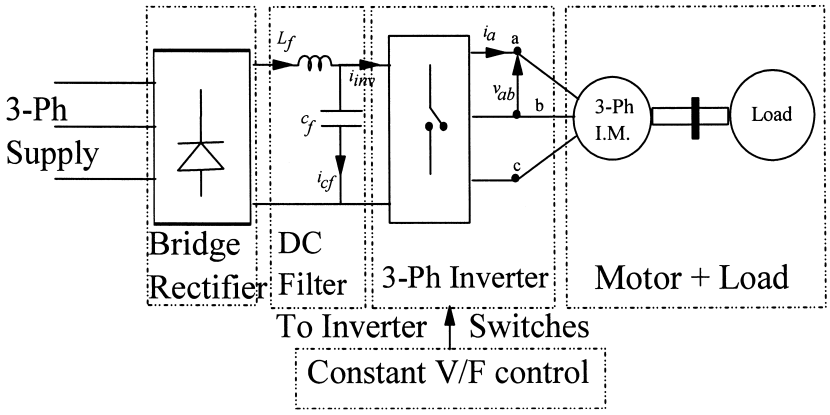

Figure 5. Constant V/F control scheme.

order filter, a three-phase bridge inverter, the large three-phase IM, and the load. The three-phase supply voltage is first rectified and a second order filter is used to smooth the voltage in the DC link. This DC voltage is converted into a three-phase AC voltage using six-step three-phase bridge inverter. The inverter switching devices are controlled such that the ratio of the fundamental component of the motor terminal voltage to its frequency is kept constant and is equal to the same ratio when the motor is supplied from rated voltage and frequency.

The following subsections present two scenarios of applying the constant V/F control scheme.

4.1. The Uncoordinated Scheme

In this scheme, the motor supply frequency, and hence its voltage, is increased in regular steps. The motor supply is increased in a step of 5 Hz with a time duration of one cycle for each frequency step. Figure 6a shows the motor developed (electric) torque while Figure 6b shows the shaft torque. Figure 6b shows that the shaft torque oscillations could reach as high as 6.2 p.u. Figure 6c shows the time variation of the magnitude of the motor line current which is given by

$$|i_s| = \sqrt{i_{ds}^2 + i_{qs}^2} \tag{6}$$

The figure shows that the motor line current could reach an undesirably high value of 9.8 p.u. Figure 6d shows that the motor takes approximately 1.0 second to reach its steady-state speed.

Figure 6 shows that the rate of increasing the supply frequency in this case is not properly set. The rated voltage has already been reached before the rotor has gained

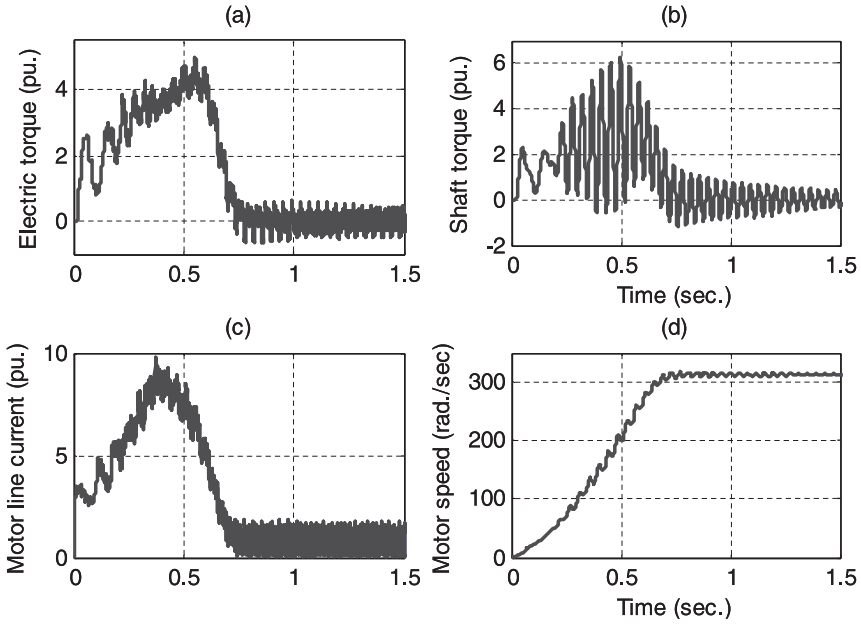

Figure 6. Motor performance with the uncoordinated constant V/F scheme.

enough speed, which results in an undesirable increase in the stator current. Furthermore, the figure show that when the torsional torque coordination is not taken into account, hazardous torsional torque may build up. In order to avoid excessive values of motor line current and guard against excitation of the mode of torsional torque oscillations, a coordinated control strategy should be adopted. This strategy is explained in the next subsection.

4.2. The Coordinated Scheme

Figure 7 shows an approximate equivalent circuit of the large motor. The motor line current is given by

$$I_s = I_2 + I_m \tag{7}$$

where I_2 is the rotor current referred to the stator circuit and I_m is the motor magnetizing current.

The rotor current, I_2, is given by

$$I_2 = \frac{V}{r_r/s + r_s + j(x_r + x_s)} \tag{8}$$

Since $r_s \ll r_r/s$, Eq. (8) can be rewritten as

$$I_2 = \frac{V}{r_r/s + j(x_r + x_s)} = \frac{s \times V}{r_r + js(x_r + x_s)} \tag{9}$$

where

$$s = \frac{\omega_s - \omega_m}{\omega_s} = \frac{\omega_r}{\omega_s}, \tag{10}$$

ω_s is the supply frequency, and
ω_r is the rotor slip frequency, and

$$x_r = \omega_s L_r, \qquad x_s = \omega_s L_s, \qquad x_m = \omega_s L_m \tag{11}$$

Equation (9) can be rewritten as

$$I_2 = \frac{\omega_r \times V/\omega_s}{r_r + j\omega_r(L_r + L_s)} \tag{12}$$

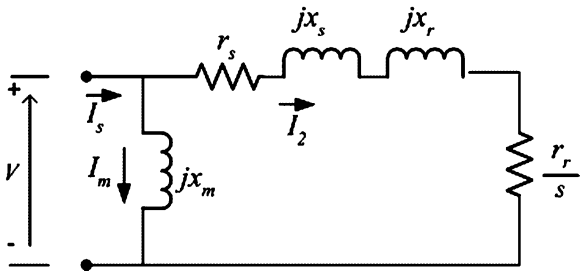

Figure 7. Equivalent circuit of the large motor.

Similarly, I_m is given by

$$I_m = \frac{V}{jx_m} = -j\frac{V/\omega_s}{L_m} \tag{13}$$

From Eqs. (7), (9), and (13), the magnitude of the motor line current can be written as

$$|I_s| = \left| \frac{\omega_r V/\omega_s}{r_r + j\omega_r(L_r + L_s)} - j\frac{V/\omega_s}{L_m} \right| \tag{14}$$

Since the ratio of V/ω_s is kept constant during the starting and the steady-state operation of the motor, the relationship between the magnitude of $|I_s|$ and ω_r is shown in Figure 8. Figure 8 is obtained by setting the ratio of V/ω_s to its value when the motor is driven using rated voltage and rated frequency, i.e.,

$$\frac{V}{\omega_s} = \frac{1 \text{ (p.u.)}}{2 \times \pi \times 50} = 3.183 \times 10^{-3} \tag{15}$$

Figure 8 shows that in order to keep the magnitude of the motor line current at a maximum of 2.0 p.u., the rotor frequency should be $\leq$16.0 rad/sec.

In order to limit the magnitude of the motor line current within a maximum of 2.0 p.u. throughout various stages of the motor operation, and to avoid exciting the torsional mode of oscillations of the large motor, the coordinated constant V/F control strategy is employed.

Figure 9 shows the proposed coordinated V/F control scheme. The operation of the scheme is carried out by starting the motor with a 10 Hz supply. This ensures that the $5f_s$-to-$7f_s$ Hz torque and the SFT components are both far from the natural torsional frequency. Also, it ensures that the fundamental component of the inverter output voltage is high enough to start the motor.

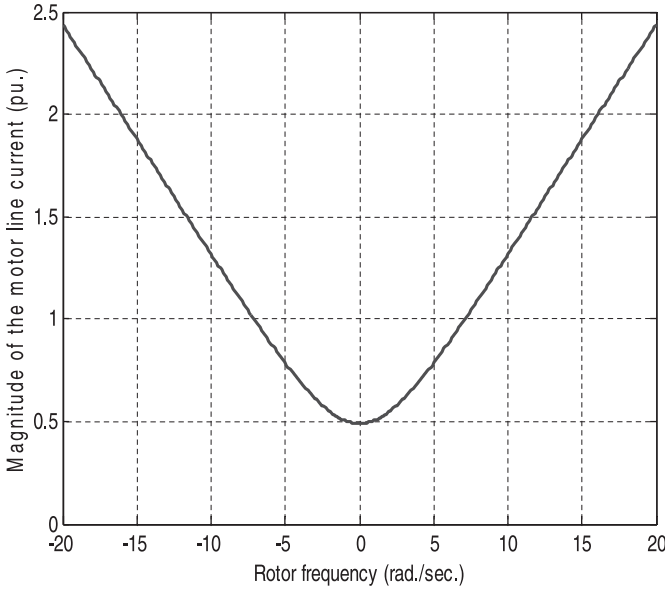

Figure 8. Relationship between magnitude of motor line current and rotor frequency.

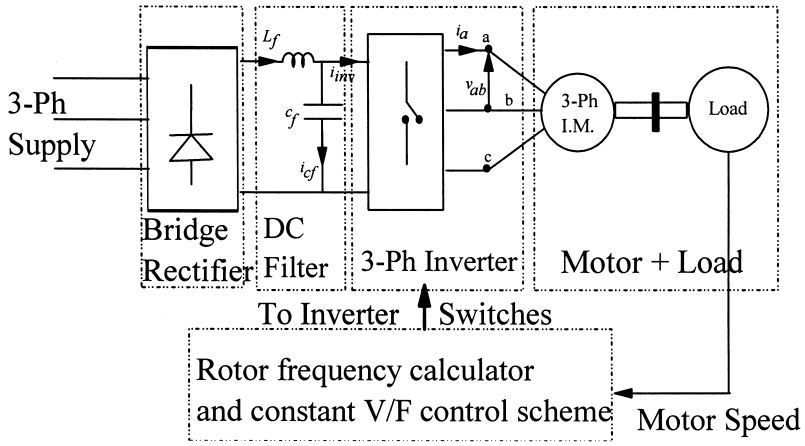

Figure 9. Coordinated constant V/F control scheme.

The inverter output frequency is kept constant until the rotor frequency becomes lower than 16 rad/sec. The inverter output frequency is then increased in a step of 1 Hz. The frequency step is kept small to minimize the transient torques associated with every step change. The motor speed is then sensed and employed in a rotor frequency calculator within the control scheme such that the rotor slip at the next operating frequency is less than 16 rad/sec. With rotor frequency kept below 16 rad/sec, the motor slip becomes less than $S_{\max}$, where $S_{\max}$ is the slip at which maximum torque takes place [8]. This ensures that the motor operates in the stable (linear) region of its torque-speed curve. Also, this mode of operation guarantees positive damping of the torsional oscillations and reduces surges in the stator current. Furthermore, a provision is made to guard against the slip frequency ($s \times f_s$) having a value coinciding with that of the natural frequency.

Figure 10 shows the time response of the motor developed torque and the shaft torque when using the coordinated constant V/F control scheme. Figure 10b shows that the maximum value of the shaft torque oscillations is 1.58 p.u. This is approximately equal to 22% of that of the direct on-line start of the motor. Figure 10c shows the magnitude of the motor line current given by Eq. (6). The figure shows that, except for the starting instant where the constant V/F scheme is not yet in effect, the coordinated scheme has been successful in keeping the magnitude of the line to its predetermined value [2.0 p.u. rms (= 2.83 p.u. peak)]. This amounts to approximately 36% of that of the direct on-line start. Figure 10d shows that the coordinated scheme takes about 3.0 seconds to bring the motor from standstill to steady-state.

5. Conclusions

This article shows that large induction motors may be subjected, in the starting period, to hazardous torsional torques in addition to high starting currents. Special consideration is given to the high torsional torques, which are usually overlooked by many drive system designers. A detailed analysis of the various torque components is presented (i) when the motor is supplied with a sinusoidal supply, and (ii) when supplied with a non-sinusoidal supply, where the problem of torsional torques is more acute.

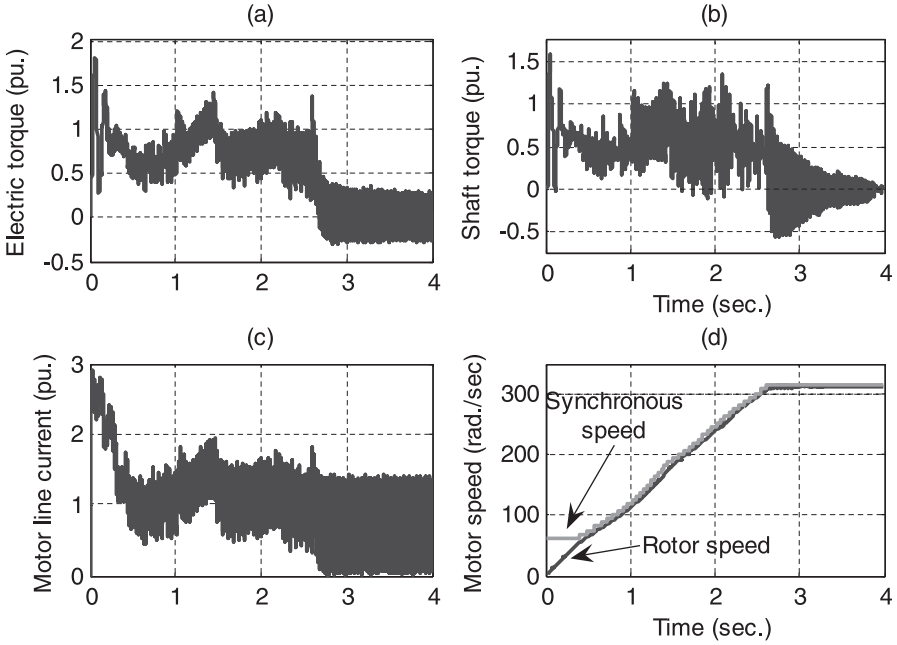

Figure 10. Motor performance with the coordinated constant V/F control scheme.

The constant V/F inverter fed motor is considered, where it is shown that improper coordination of this scheme may result in high starting currents and torsional torques. Hence, this article presented a coordinated V/F scheme that counteracts both problems. The proposed control strategy is explained and its capability is verified. Computer simulation of the motor under study shows that, with proper coordination, the value of the torsional torque oscillations is reduced to 22% of that of the direct on-line start and the value of the starting current is limited to 36% of that of the direct on-line start.

6. Appendix: System Parameters

The following system parameters are given in p.u.

6.1. Electric Motor Data

1000 hp, 2300 V, 50 Hz, 1483 rpm
$x_m = 2.042$, $x_{ss} = 2.1195$, $x_{rr} = 2.0742$, $r_s = 0.0453$, $r_r = 0.0272$.

6.2. Mechanical Data

$D_{ml} = 0.002$, $D_m = 0.0$, $D_l = 0.0$, $H_m = 0.3$ s, $H_l = 0.75$ s, $K_s = 30.0$ p.u./rad, $T_l = 0.0$.

References

1. J. Nevelsteen and H. Aragon, "Starting of large motors—methods and economics," *IEEE Transactions on Industry Applications*, Vol. 25, No. 6, pp. 1012–1018, November/December 1989.

2. J. H. Stout, "Capacitor starting of large motors," *IEEE Transactions on Industry Applications*, Vol. IA-14, No. 3, pp. 209–212, May/June 1978.
3. A. Shaltout, "Analysis of torsional torques in starting of large squirrel cage induction motors," *IEEE Transactions on Energy Conversion*, Vol. 9, No. 1, pp. 135–142, March 1994.
4. N. Abdel-Rahim and A. Shaltout, "Suppression of torsional torque oscillations in starting large squirrel cage induction motors using slip-frequency control," *Ninth International Middle-East Power Conference (MEPCON 2003)*, Menoufia, Egypt, December 16–18, 2003.
5. P. C. Krause, O. Wasynczuk, and S. D. Sudhoff, *Analysis of Electric Machinery and Drive Systems*, New York: IEEE Press, 2002.
6. C.-M. Ong, *Dynamic Simulation of Electric Machinery Using MATLAB/ SIMULINK*, Upper Saddle River, NJ: Prentice Hall, 1998.
7. C. B. Mayer, "Torsional vibration problems and analyses of cement industry drive," *IEEE Transaction on Industry Applications*, Vol. IA-17, No. 1, pp. 81–89, January/February 1981.
8. S. J. Chapman, *Electric Machinery Fundamentals*, New York: McGraw-Hill International edition, 1999.